Modelling of Hydrogen Tank Fuelling

Dadashzadeh M.*, Makarov D., Molkov V.

HySAFER, Ulster University, Belfast School of Architecture and the Built Environment, Newtownabbey, Co. Antrim, UK
**Corresponding author's email: s.dadashzadeh@ulster.ac.uk*

ABSTRACT

A model to simulate thermal behaviour of an onboard storage tank and parameters of hydrogen inside the tank during fuelling is presented. The energy conservation equation, Abel-Noble real gas equation of state, and the entrainment theory are applied in the model to reproduce the experimentally recorded dynamics of hydrogen temperature inside the tank and distribution of temperature through the wall. Convective heat transfer between hydrogen, tank wall and the atmosphere are modelled using Nusselt number correlations. An original methodology, based on the entrainment theory, is devised to calculate changing velocity of the gas inside the tank during the fuelling. Conductive heat transfer through the tank wall, composed of load-bearing carbon fibre reinforced polymer and a layer of liner, is modelled by employing one-dimensional unsteady heat transfer equation. The model is validated against experiments on fuelling of Type III and IV composite tanks for onboard hydrogen storage. Hydrogen temperature inside a tank is predicted by the model within the experimental non-uniformity of 5^0C.

KEYWORDS: Hydrogen fuelling, model, validation, fuelling protocol.

NOMENCLATURE

A_{int}	Internal tank surface (m^2)
b	Co-volume constant for hydrogen in Abel-Noble equation (m^3/kg)
$c_{p,\,air}$	Specific heat capacity of air at constant pressure (J/kg/K)
$c_{p,g}$	Specific heat capacity of the inside gas at constant pressure (J/kg/K)
$c_{p,wall}$	Specific heat capacity of the tank wall (CFRP: $c_{p\ wall\ (CFRP)}$; liner: $c_{p\ wall\ (liner)}$) (J/kg/ K)
Dext	External tank diameter (m)
D_{inlet}	Nozzle diameter (m)
D_{int}	Internal tank diameter (m)
f	Friction factor (-)
Gr_{tank}	Grashof number (-)
g	Gravity acceleration (m/s^2)
h_{in}	Enthalpy of gas entering the tank (J/kg)
k_{ext}	Convective heat transfer coefficient at external surface of tank wall ($W/m^2/K$)
$k_{int\ forced}$	Convective heat transfer coefficient
Pr	Prandtl number of gas inside tank (-)
Q	Heat into tank from surrounding (J)
R_{H_2}	Hydrogen gas constant ($m^2\ s^2/K$)
Re_{tank}	Effective Reynolds number inside tank (-)
T_{amb}	Ambient temperature (K)
T_{tank}	Temperature of gas inside tank (K)
$T_{wall\ (ext)}$	Temperature of tank external surface (K)
$T_{wall(int)}$	Temperature of tank internal surface (K)
T_{del}	Delivery temperature of gas during fuelling (K)
T^0_{tank}	Initial temperature of gas inside tank (K)
$T_{wall\ (n)}$	Temperature of tank wall at the grid-point "n" (K)
T^0_{wall}	Initial temperature of tank wall (K)
t	Time (s)

Proceedings of the Ninth International Seminar on Fire and Explosion Hazards (ISFEH9), pp. 1395-1406
Edited by Snegirev A., Liu N.A., Tamanini F., Bradley D., Molkov V., and Chaumeix N.
Published by Saint-Petersburg Polytechnic University Press
ISBN: 978-5-7422-6498-9 DOI: 10.18720/spbpu/2/k19-20

	at external surface of tank wall (forced convection) (W/ m2/K)
$k_{int\ natural}$	Convective heat transfer coefficient at internal surface of tank wall (natural convection) (W/m2/K)
k_{int}	Convective heat transfer coefficient at internal surface of tank wall (W/m^2/K)
L	Internal tank length (m)
$\dot{m}_{ent}$	Entrainment mass flow rate (kg/s)
$\dot{m}_{inlet}$	Inlet mass flow rate (kg/s)
$\dot{m}^0_{inlet}$	Initial inlet mass flow rate (kg/s)
M_0	Momentum flux (m/kg/s2)
m_{ent}	Mass of gas at entrainment
m_{inlet}	Mass of gas at inlet (in considerations of kinetic energy) (kg)
m_{tank}	Mass of gas in tank (kg)
m^0_{tank}	Initial mass of gas in tank (kg)
$Nu_{int\ natural}$	Nusselt number for natural convection (-)
$Nu_{int\ forced}$	Nusselt number for forced convection (-)
P_{tank}	Pressure of gas inside tank (Pa)
P^0_{tank}	Initial pressure of gas inside tank (Pa)
u_{ent}	Gas velocity due to entrainment (m/s)
u_{inlet}	Inlet gas velocity (m/s)
u_{tank}	Tank gas velocity (m/s)
U	Total internal energy in tank (J)
V	Tank volume (m3)
Z	Hydrogen compressibility factor (-)

Greek

β	Thermal expansion coefficient of gas (1/K)
γ	Specific heats ratio (-)
λ_g	Thermal conductivity of gas (W/m/K)
μ_g	Dynamic viscosity of gas (Pa s)
μ_{air}	Viscosity of air (Pa s)
λ_{air}	Thermal conductivity of air (W/m/K)
ρ_{air}	Density of air (kg/m3)
λ_{wall}	Thermal conductivity of tank wall (CFRP: $\lambda_{wall\ (CFRP)}$; liner: $\lambda_{wall\ (liner)}$) (W/m/K)
ρ^0_{tank}	Initial gas density inside tank (kg/m3)
ρ_{inlet}	Gas density at inlet (kg/m3)
ρ_{tank}	Gas density inside tank (kg/m3)
ρ_{wall}	Tank wall density (CFRP: $\rho_{wall\ (CFRP)}$; liner: $\rho_{wall\ (liner)}$) (kg/m3)

INTRODUCTION

The inherently safer fuelling of onboard hydrogen composite storage container is a challenging problem. Independent on tank design and materials used for load bearing wall and liner, tank's volume, its initial and nominal working pressure (NWP), temperature of hydrogen supplied to tank, the regulation and standards [1–4] require that the temperature inside the tank does not exceed 85^0C and pressure does not exceed 1.25×NWP, i.e. 87.5 MPa for 70 MPa onboard storage tanks. The consumer expectations include the fuelling time of hydrogen-powered passenger car within 3 min. Longer fuelling time is acceptable for busses. The problem of fuelling control is complicated by changing pressure and temperature inside the tank and at the inlet, changing diameter of fuelling nozzle to keep a required pressure ramp profile, requirements to the fuelling time, conjugate heat transfer from/to hydrogen through a tank wall to/from the ambience, use of wall and liner materials of different thermal conductivity, thermal capacity, etc.

Experimental investigation of hydrogen fuelling for arbitrary conditions is expensive. Up to now experimental studies did not yet end up by clear and transparent fuelling protocol. Computational fluid dynamics (CFD) is a contemporary research method to get insights into underlying physical phenomena. It helps as well to avoid carrying out hazardous and expensive experiments. CFD studies on hydrogen fuelling are extensive [5–14]. However, CFD simulations are not always time efficient [15] and hardly could be used as a part of automated fuelling system with a short response time.

Hydrogen fuelling models and their applications can be found elsewhere [7,15–21]. A major drawback in these studies is a lack of universal approach for estimation of heat transfer coefficient.

The convective heat transfer on a tank walls depends on the heat transfer coefficient [22,23]. The universal modelling approach to estimate this coefficient is vital [21].

The aim of this study is to develop and validate a model to better understand and reproduce the underlying phenomena of onboard hydrogen tank fuelling. The model can be used as a basis for creation of a predictive tool for the thermal behaviour of the system dispenser-hydrogen-tank-atmosphere during fuelling.

MODEL

The schematic diagram of the hydrogen storage tank during the fuelling and phenomena on its boundaries are presented in Fig. 1.

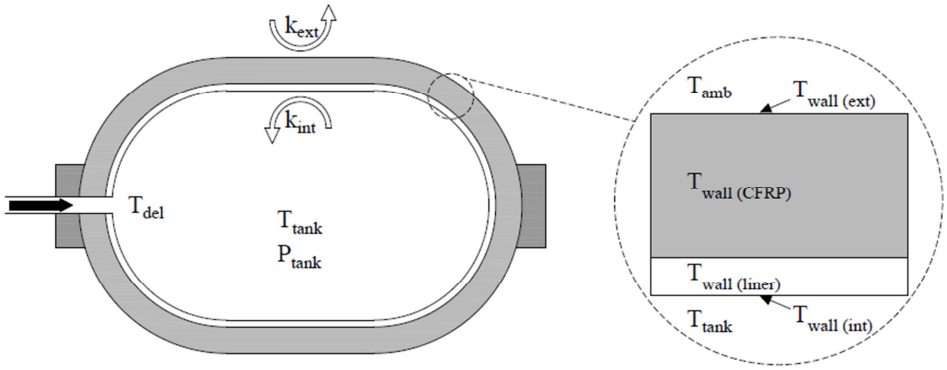

Fig. 1. Scheme of a tank and related phenomena during fuelling.

Hydrogen thermodynamic parameters during fuelling are related through Abel-Noble real gas equation of state (EOS) [24]

$$P_{tank} = Z\rho_{tank}R_{H_2}T_{tank}, \tag{1}$$

where $Z = 1/(1 - b\rho_{tank})$ is the compressibility factor.

The first law of thermodynamic is used in the model to bring together the rate of change of internal energy of hydrogen in the tank, rate of heat transfer to/from hydrogen through the tank wall, composed of a composite polymer and a liner with different thermodynamic parameters, and the rate of enthalpy brought into the tank by hydrogen inflow

$$\frac{dU}{dt} = \frac{dQ}{dt} + h_{in}\frac{dm_{tank}}{dt}, \tag{2}$$

where the enthalpy of the gas entering (delivered into) the tank is realised as $h_{in} = c_{p,g}T_{del}$.

The internal energy of real gas is calculated similar to [25] as

$$U = \frac{P_{tank}(V - m_{tank}b)}{\gamma - 1}. \tag{3}$$

The rate of heat transfer can be modelled as elsewhere, e.g. [19],

$$\frac{dQ}{dt} = k_{int}A_{int}\left(T_{wall(int)} - T_{tank}\right), \tag{4}$$

where T_{tank} is the gas temperature inside the tank in the assumption of its uniformity. The criteria to define the regime of convective heat transfer (natural convection, forced convection, or combined regime) is defined as [26]

$$\begin{cases} If\ \dfrac{Gr_{tank}}{(Re_{tank})^2} < 0.1, \quad k_{int} = k_{int\,forced}, & (5) \\ If\ 0.1 \le \dfrac{Gr_{tank}}{(Re_{tank})^2} \le 10, \quad k_{int} = \left(k_{int\,natural}{}^4 + k_{int\,forced}{}^4\right)^{\frac{1}{4}}, & (6) \\ If\ \dfrac{Gr_{tank}}{(Re_{tank})^2} > 10, \quad k_{int} = k_{int\,natural}, & (7) \end{cases}$$

where Grashof number, Gr_{tank}, is calculated as

$$Gr_{tank} = \frac{g\beta\left|T_{tank} - T_{wall(int)}\right|\rho_{tank}^2 D_{int}^3}{\mu_g{}^2}. \quad (8)$$

Gas thermal properties, i.e. thermal conductivity (λ_g); specific heat capacity ($c_{p,g}$); viscosity (μ_g), extracted for different pressure and temperature were interpolated based on gas pressure and temperature from [27].

The values of heat transfer coefficients $k_{int\,forced}$ and $k_{int\,natural}$ are calculated as a function of Nusselt number, internal tank diameter, and gas thermal conductivity which is interpolated for different pressure and temperature from [27], respectively as

$$k_{int\,natural} = \frac{\lambda_g \times Nu_{int\,natural}}{D_{int}}, \quad (9)$$

$$k_{int\,forced} = \frac{\lambda_g \times Nu_{int\,forced}}{D_{int}}. \quad (10)$$

Natural convection Nusselt number, $Nu_{int\,natural}$, is calculated by the empirical equation [18]

$$Nu_{int\,natural} = 0.104 \times \left(\frac{g\beta\left|T_{tank} - T_{wall(int)}\right|c_{p,g}(\rho_{tank})^2 D_{int}^3}{\mu_g \lambda_g}\right)^{0.352}. \quad (11)$$

Forced convection Nusselt number, $Nu_{int\,forced}$, is calculated using the correlation [26]

$$Nu_{int\,forced} = \frac{(f/8)(Re_{tank} - 1000)Pr}{1 + 12.7(f/8)^{0.5}\,(Pr^{2/3} - 1)}, \quad (12)$$

where the friction factor, f, and Prandtl number, Pr, inside the tank are calculated by the following correlation [26] and definition respectively

$$f = (0.790 \cdot ln\, Re_{tank} - 1.64)^{-2}, \quad (13)$$

$$Pr = \frac{\mu_g \cdot c_{p,g}}{\lambda_g}. \quad (14)$$

Reynolds number inside the tank for calculation of the friction factor and Nusselt number for forced convection is

$$Re_{tank} = \frac{\rho_{tank} u_{tank} D_{int}}{\mu_g}. \quad (15)$$

The original modelling approach is applied in this study to calculate characteristic velocity of hydrogen in a tank. It is based on the entrainment theory [28]. The procedure is as follows. The density of hydrogen at inlet is calculated using Abel-Noble EOS

$$\rho_{inlet} = \frac{P_{tank}}{P_{tank} b + R_{H_2} T_{del}}. \quad (16)$$

The inlet velocity is calculated by the mass flow rate

$$u_{inlet} = \frac{4\dot{m}_{inlet}}{\rho_{inlet} (D_{inlet})^2 \pi}. \quad (17)$$

Using the inlet density, ρ_{inlet}, and inlet velocity, u_{inlet}, the momentum flux, M_0, and the entrainment mass flow rate inside the tank, $\dot{m}_{ent}$, are calculated respectively as [28]

$$M_0 = \frac{1}{4}\pi (D_{inlet})^2 \rho_{inlet} (u_{inlet})^2, \quad (18)$$

$$\dot{m}_{ent} = 0.282 (M_0)^{0.5} (\rho_{tank})^{0.5} L. \quad (19)$$

Then, the velocity of hydrogen in the tank due to the process of entrainment can be calculated as

$$u_{ent} = \frac{4\dot{m}_{ent}}{\rho_{tank} (D_{int})^2 \pi}. \quad (20)$$

To calculate a characteristic velocity inside the tank, u_{tank}, the kinetic energy of hydrogen entering the tank and the kinetic energy of hydrogen moving inside the tank due to entrainment, are added

$$\frac{m_{tank} (u_{tank})^2}{2} = \frac{m_{ent} (u_{ent})^2}{2} + \frac{m_{inlet} (u_{inlet})^2}{2}. \quad (21)$$

Considering that all hydrogen inside the tank is involved in the movement due to the entrainment phenomenon, i.e. $m_{ent} = m_{tank}$, and using the definition $m_{inlet} = \dot{m}_{inlet} \Delta t$, this equation can be solved for the characteristic velocity for use in the calculation of Reynolds number as

$$u_{tank} = \left[\frac{m_{tank} (u_{ent})^2 + m_{inlet} (u_{inlet})^2}{m_{tank}} \right]^{1/2}. \quad (22)$$

Differentiating Eq. (3) and considering the rate of heat transfer, defined by Eq. (4), the differencial equation for calculation of hydrogen mass in the tank (m_{tank}) is obtained from Eq. (2)

$$\frac{dm_{tank}}{dt} = \frac{\frac{dP_{tank}}{dt} \frac{(V - m_{tank} \cdot b)}{\gamma - 1} - k_{int} A_{int} (T_{wall(int)} - T_{tank})}{\frac{P_{tank}}{\gamma - 1} \cdot b + c_{p,g} \cdot T_{del}}. \quad (23)$$

The density is calculated as $\rho_{tank} = \frac{m_{tank}}{V}$ and it is followed by using Eq. (24) [24] to calculate the temperature of the hydrogen inside the tank in the assumption of uniformity of hydrogen parameters throughout the tank (T_{tank})

$$T_{tank} = \frac{P_{tank} (1 - b\rho_{tank})}{\rho_{tank} R_{H_2}}. \quad (24)$$

Conservation of energy requires the equality of the convective heat flux between gas and the wall to the conductive heat flux at the wall boundary. Thus, boundary conditions at internal and external surfaces of the tank are defined by Eq. (25) and Eq. (26) respectively

$$q''_{conduction}\ \ (internal) = q''_{convection} \Rightarrow -\lambda_{wall}\left.\frac{dT_{wall\,(n)}}{dx}\right|_{n=int} = k_{int}\left(T_{tank} - T_{wall\,(int)}\right), \quad (25)$$

$$q''_{conduction}\ \ (external) = q''_{convection} \Rightarrow -\lambda_{wall}\left.\frac{dT_{wall\,(n)}}{dx}\right|_{n=ext} = k_{ext}\left(T_{wall\,(ext)} - T_{amb}\right). \quad (26)$$

It was concluded in [9,19,29] that in the case of fuelling, the external heat transfer coefficient (k_{ext}) does not have a significant effect. The value of k_{ext} is then accepted to be 6 W/m^2/K in our study following [9].

The model implies the unsteady heat conduction inside the cylinder wall. The equation per each control volume (CV) of the wall can be found elsewhere [30]

$$\rho_{wall} c_{p\,wall}\frac{dT_{wall}}{dt} = \frac{d}{dx}\left(\lambda_{wall}\frac{dT_{wall}}{dx}\right). \quad (27)$$

The model input parameters are defined as the following categories:

- Tank properties: volume, internal surface, diameter & length, external diameter, load-bearing wall and liner thickness and their thermal properties (thermal conductivity, specific heat capacity, density), external heat transfer coefficient; nozzle diameter, initial temperature,
- Hydrogen properties: co-volume constant, specific heat capacity, thermal conductivity, specific gas constant, dynamic viscosity, initial pressure and temperature, pressure ramp, delivery temperature, thermal expansion coefficient, specific heat capacities ratio,
- Other input parameters: ambient temperature, air specific heat capacity, air viscosity, air thermal conductivity, air density, fuelling time, acceleration due to gravity.

The model can predict the dynamics of gas temperature inside the tank, the temperature profile within the load bearing wall and the liner, the gas density or State of Charge (SOC), etc.

Input parameters, order of equations which are solved at each time step, and expected output of calculation at each stage are summarised in Table 1. It must be noted that $\frac{dP_{tank}}{dt}$ is the pressure ramp which is defined as an input.

Two hydrogen tank fuelling experiments [8,29] were selected for the validation of the physical model of fuelling developed in this study. Table 2 presents the characteristics of the tanks in these experiments. The details of experiments were out of scope of the current study and they are available in [8] for the 29 L, Type IV tank and in [29] for the 74 L, Type III tank. According to [8], for 29 L, Type IV tank, the measurement for the gas temperature inside the tank was facilitated by 8 thermocouples. It was concluded in [8,10] that five out of 8 thermocouples, i.e. in the middle of the tank from top to bottom, were assigned to be used for the averaging the temperature due to having same temperature trend with the maximum temperature difference of 3^{0}C. Sixteen thermocouples were used to measure the gas temperature inside the 74 L, Type III tank of [29] experiment. Unfortunately, there was no argument in [29] that how the temperatures were averaged and it was only mentioned that the maximum difference of gas temperature measured by different thermocouples was 5^{0}C.

Table 1. Input parameters, calculation procedure and output parameters

Input parameters	
V, b, γ, T_{amb}, T_{del}, $\frac{dP_{tank}}{dt}$, T^0_{tank}, T^0_{wall}, A_{int}, Δx, Δt, R_{H_2}, $\rho_{wall(n)}$, $c_{p\,wall(n)}$, λ_{wall}, k_{ext}, D_{int}, L, g, β, T^0_{wall}, k^0_{int}, $c_{p,g}$, μ_g, λ_g, ρ^0_{tank}, m^0_{tank}	
Calculation procedures	
Step No.	Output parameters
1	Hydrogen pressure in the tank, ($P^i_{tank} = P^{i-1}_{tank} + \left(\frac{dP_{tank}}{dt}\right)\Delta t$)
2	Hydrogen mass flow rate in tank ($\dot{m}^i_{inlet} = \frac{dm_{tank}}{dt}$), Eq. (23)
3	Hydrogen mass in tank ($m^i_{tank} = m^{i-1}_{tank} + dm_{tank}$)
4	Hydrogen density in tank ($\rho_{tank} = \frac{m_{tank}}{V}$)
5	Hydrogen temperature in tank (T_{tank}), Eq. (24)
6	Temperature of wall control volumes ($T_{wall\,(n)}$), Eq. (27)
7	Temperature of wall internal surface ($T_{wall\,(int)}$), Eq. (25)
8	Temperature of wall external surface ($T_{wall\,(ext)}$), Eq. (26)
9	Hydrogen density at inlet (ρ_{inlet}), Eq. (16)
10	Hydrogen velocity at inlet (u_{inlet}), Eq. (17)
11	Momentum flux at inlet (M_0), Eq. (18)
12	Entrained mass flow rate ($\dot{m}_{ent}$), Eq. (19)
13	Velocity of entrained gas (u_{ent}), Eq. (20)
14	Hydrogen mass passing inlet during time step Δt ($m_{inlet} = \dot{m}_{inlet}\Delta t$)
15	Hydrogen mass participating in entrainment ($m_{ent} = m_{tank}$), used in Eq. (21)
16	Hydrogen velocity in tank (u_{tank}), Eq. (21)
17	Reynolds number of hydrogen flow in tank (Re_{tank}), Eq. (15)
18	Friction coefficient for flow in tank (f), Eq. (13)
19	Prandtl number in tank (Pr), Eq. (14)
20	Natural convection Nusselt number ($Nu_{int\,natural}$), Eq. (11)
21	Forced convection Nusselt number ($Nu_{int\,forced}$), Eq. (12)
22	Natural convection heat transfer coefficient ($k_{int\,natural}$), Eq. (9)
23	Forced convection heat transfer coefficient ($k_{int\,forced}$), Eq. (10)
24	Grashof number (Gr_{tank}), Eq. 8
25	Internal surface heat transfer coefficient (Eq. (5) or Eq. (6) or Eq. (7)),
26	Repeating steps 1 to 25 as long as $T_{tank} < 85^0C$ *or* $P_{tank} < 1.25 \times$ NWP *or* $SOC \leq 100\%$.

VALIDATION EXPERIMENTS

Table 2. Characteristics of tanks used in validation experiments [8,14,29]

Characteristics	Type IV	Type III
Reference	[8]	[29]
Volume (L)	29	74
External length (mm)	827	1030
External diameter (mm)	279	427
Internal diameter (mm)	230	354
Liner material	HDPE*	AA*
$\lambda_{wall\ (liner)}$ (W/m/K)	0.385	238
$c_{p\ wall\ (liner)}$ (J/kg/K)	1580	902
$\rho_{wall\ (liner)}$ (kg/m^3)	945	2700
Composite shell material	CFRP	CFRP
$\lambda_{wall\ (CFRP)}$ (W/m/K)	0.74	0.612
$c_{p\ wall\ (CFRP)}$ (J/kg/K)	1120	840
$\rho_{wall\ (CFRP)}$ (kg/m^3)	1494	1570
Injector diameter (mm)	3	5
Ambient temperature (K)	293	303
Initial temperature (K)	293	288
Gas delivery temperature (K)	298	298
Initial pressure (MPa)	2	5.5
Target pressure (MPa)	77	70
Filling time (s)	250	640

* HDPE: High density polyethylene; AA: Aluminium alloy;
CFRP: Carbon fibre reinforced polymer.

RESULTS AND DISCUSSION

Figures 2 and 3 demonstrate the comparison of simulation results obtained by the developed physical model against the validation experiments for 29 L Type IV tank [8] and 74 L Type III tank [29]. The pressure ramp used in each experiment is also presented with small graph on the right bottom of each figure.

The temperature dynamics by the physical model is in good agreement with measured in the experiments temperature [8,29].

In the case of the smallest tank of volume 29 L (Fig. 2), the model slightly underpredicts the experimental temperature at the beginning of the process (0-60 s), and the calculations are more accurate to the end of the fuelling.

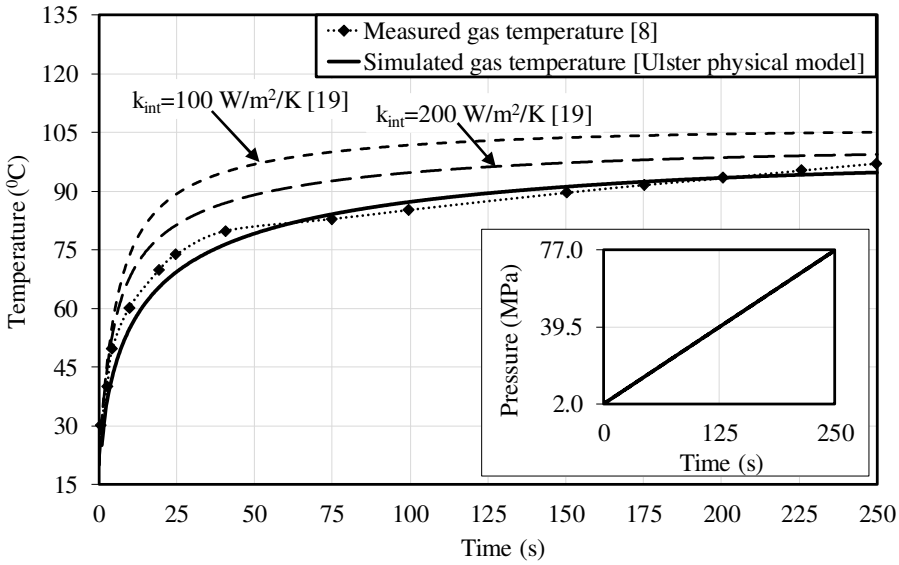

Fig. 2. Experimental and calculated temperature dynamics for the Type IV tank, 29 L [8].

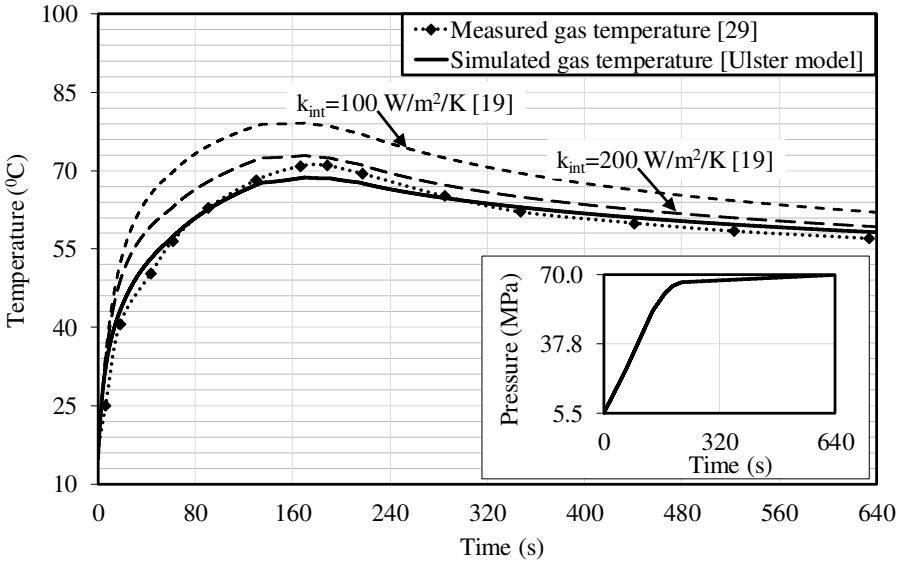

Fig. 3. Experimental and calculated temperature dynamics for the Type III tank, 74 L [29].

The relative deviation between the simulation and experimental results are observed in Fig. 2. The maximum deviation of the simulation results from the experiment is 5^0C. The maximum experimental temperature difference in the tank is 3^0C [10]. This proves that the simulation results are in a good agreement with the experimental data. Two more simulations were also performed with constant k_{int} of 100 W/m^2/K and 200 W/m^2/K following the study of [19]. As presented in Fig. 2, simulations with constant k_{int} of [19] overpredict the temperature of the gas inside the tank, i.e. 10^0C and 15^0C overprediction by using k_{int} of 100 W/m^2/K and 200 W/m^2/K respectively. The effect of employing entrainment theory in our modeling approach is obvious, i.e. dynamic

calculation of the internal heat transfer coefficient (k_{int}) following by accurate prediction of the gas temperature inside the tank.

In the case of the largest 74 L volume Type III tank (Fig. 3), the model slightly overpredicts at the beginning, but then slightly underpredicts when the simulation continues until the end of fuelling. This third validation experiment has changing during fuelling pressure ramp compared to constant but different pressure ramps in the first and the second validation tests. The pressure ramp is significantly higher at the beginning of the fuelling and the pressure ramp slope reduces significantly after around 160-180 s. The result is the temperature peak in the temperature dynamics. One may observe the relative deviation between the simulation results and experiment in Fig. 3. The maximum deviation of the simulation in is again 3^0C. According to [29], the maximum experimental difference in the tank is 5^0C which makes an excellent agreement between the simulation results and those obtained by the experiment. It is worth noting that the model reproduced the temperature peak. The impact of Ulster approach in employing entrainment theory for the estimation of $k_{int}$is again obvious in Fig. 3. While using constant k_{int} of 100 W/m^2/K and 200 W/m^2/K, following the study of [19], overpredicts the inside temperature of the gas, our model simulates the gas temperature inside the tank within an acceptable level of accuracy.

CONCLUSIONS

The significance of this study is in the development of the model accounting for underlying phenomena during hydrogen fuelling of composite onboard high-pressure cylinders that can be used for development of automated hydrogen fuelling protocols for light- and heavy-duty vehicles. The model provides the parameters for the regulatory control of the thermal behaviour of the tank during the fuelling, including but not limited to gas temperature, gas density or state of charge (SOC), etc. The rigour of the study is in the model validation against experimental data on fuelling of hydrogen storage tanks of Type III and Type IV with the volumes of 29 L and 74 L, respectively up to pressure 77 MPa with constant and changing fuelling pressure ramp. The model reproduced experimental temperatures within acceptable maximum value of 5^0C characteristic for hydrogen temperature non-uniformity in fuelling tests. The originality of this study is based on integrating physics and thermodynamic methods and correlations in an engineering application to achieve the synergy through their complementarities. The cornerstone of the model is the use of the entrainment theory in combination with conservation of kinetic energy for calculation of gas velocity inside the tank to calculate Reynolds number used in estimation of the Nusselt number and thus the heat transfer coefficient for convective heat transfer between the tank wall and the gas.

ACKNOWLEDGEMENT

The authors are grateful to UK Engineering and Physical Sciences Research Council (EPSRC) for funding through EPSRC SUPERGEN H2FC Hub (EP/J016454/1 and EP/P024807/1) and EPSRC SUPERGEN Challenge “Integrated safety strategies for onboard hydrogen storage” (EP/K021109/1) projects. This study has received funding from the Fuel Cell and Hydrogen 2 Joint Undertaking under grant agreement No.736648 (NET-Tools project). This Joint Undertaking received support from the European Union’s Horizon 2020 research and innovation programme and Hydrogen Europe (HE) and Hydrogen Europe Research (HER). This research is supported by the Project “HYLANTIC”–EAPA_204/2016 which is co-financed by the European Regional Development Found in the framework of the Interreg Atlantic programme.

REFERENCES

[1] GTR ECE/TRANS/WP.29/2013/41, Global technical regulation (GTR) on hydrogen and fuel cell vehicles, (2013).

[2] Commission Regulation No 406/2010, Implementing Regulation (EC) No 79/2009 of the Parliament and of the Council on type-approval of hydrogen-powered vehicles, Off. J. Eur. Union. (2010).

[3] SAE J2601, Fueling protocols for light duty gaseous hydrogen surface vehicles, SAE Int. (2016).

[4] SAE J2579_201806, Standard for Fuel Systems in Fuel Cell and Other Hydrogen Vehicles, SAE Int. Detroit MI, U.S. (2018).

[5] T. Bourgeois, F. Ammouri, D. Baraldi, P. Moretto, The temperature evolution in compressed gas filling processes: A review, Int. J. Hydrogen Energy 43 (2018) 2268–2292.

[6] D. Melideo, D. Baraldi, N. De Miguel Echevarria, B. Acosta Iborra, Effects of the injector directions on the temperature distribution during filling of hydrogen tanks, in: 7th Int. Conf. Hydrog. Saf. (ICHS 2017), 2017.

[7] T. Bourgeois, T. Brachmann, F. Barth, F. Ammouri, D. Baraldi, D. Melideo, B. Acosta-Iborra, D. Zaepffel, D. Saury, D. Lemonnier, Optimization of hydrogen vehicle refuelling requirements, Int. J. Hydrogen Energy 42 (2017) 13789–13809.

[8] N. de Miguel, B. Acosta, D. Baraldi, R. Melido, R. Ortiz Cebolla, P. Moretto, The role of initial tank temperature on refuelling of on-board hydrogen tanks, Int. J. Hydrogen Energy 41 (2016) 8606–8615.

[9] I. Simonovski, D. Baraldi, D. Melideo, B. Acosta-Iborra, Thermal simulations of a hydrogen storage tank during fast filling, Int. J. Hydrogen Energy 40 (2015) 12560–12571.

[10] R. Ortiz Cebolla, B. Acosta, P. Moretto, N. Frischauf, F. Harskamp, C. Bonato, D. Baraldi, Hydrogen tank first filling experiments at the JRC-IET GasTeF facility, Int. J. Hydrogen Energy 39 (2014) 6261–6267.

[11] D. Melideo, D. Baraldi, M.C. Galassi, R. Ortiz Cebolla, B. Acosta Iborra, P. Moretto, CFD model performance benchmark of fast filling simulations of hydrogen tanks with pre-cooling, Int. J. Hydrogen Energy 39 (2014) 4389–4395.

[12] M. Heitsch, D. Baraldi, P. Moretto, Numerical investigations on the fast filling of hydrogen tanks, Int. J. Hydrogen Energy 36 (2011) 2606–2612.

[13] N. de Miguel, R. Ortiz Cebolla, B. Acosta, P. Moretto, F. Harskamp, C. Bonato, Compressed hydrogen tanks for on-board application: Thermal behaviour during cycling, Int. J. Hydrogen Energy 40 (2015) 6449–6458.

[14] B. Acosta, P. Moretto, N. de Miguel, R. Ortiz, F. Harskamp, C. Bonato, JRC reference data from experiments of on-board hydrogen tanks fast filling, Int. J. Hydrogen Energy 39 (2014) 20531–20537.

[15] T. Bourgeois, F. Ammouri, M. Weber, C. Knapik, Evaluating the temperature inside a tank during a filling with highly-pressurized gas, Int. J. Hydrogen Energy 40 (2015) 11748–11755.

[16] M. Monde, Y. Mitsutake, P. Woodfield, S. Maruyama, Characteristics of heat transfer and temperature rise of hydrogen during rapid hydrogen filling at high pressure, Heat Transf. Res. 36 (2006) 13–27.

[17] P.L. Woodfield, T. Takano, M. Monde, Characteristics of heat transfer for hydrogen and wall during filling hydrogen into actual tank at high pressure, in: Asme/Jsme Therm. Eng. Summer Heat Transf. Conf., 2007: pp. 1069–1076.

[18] P.L. Woodfield, M. Monde, T. Takano, Heat tranfer charateristics for practical hydrogen vessels being filled at high pressure, J. Therm. Sci. Technol. 3 (2008) 241–253.

[19] M. Monde, P. Woodfield, T. Takano, M. Kosaka, Estimation of temperature change in practical hydrogen pressure tanks being filled at high pressures of 35 and 70 MPa, Int. J. Hydrogen Energy 37 (2012) 5723–5734.

[20] M. Monde, M. Kosaka, Understanding of Thermal Characteristics of Fueling Hydrogen High Pressure Tanks and Governing Parameters, SAE Int. J. Altern. Powertrains. 2 (2013) 61–67.

[21] P.L. Woodfield, M. Monde, Y. Mitsutake, Measurement of average heat tranfer coefficients in high-pressure vessel during charging with hydrogen, nitrogen or argon gas, J. Therm. Sci. Eng. 2 (2007) 180–190.

[22] R.W. Schefer, W.G. Houf, T.C. Williams, B. Bourne, J. Colton, Characterization of high-pressure, underexpanded hydrogen-jet flames, Int. J. Hydrogen Energy 32 (2007) 2081–2093.

[23] M. Dadashzadeh, D. Makarov, V. Molkov, Non-adiabatic blowdown model: a complimentary tool for the safety design of tank-TPRD system, in: Int. Conf. Hydrog. Safety, Sept. 11-13, 2018, Hamburg, Ger., 2017.

[24] I. Johnson, The Noble-Abel equation of state: thermodynamic derivations for ballistics modelling, 2005.

[25] V. Molkov, S. Kashkarov, Blast wave from a high-pressure gas tank rupture in a fire: Stand-alone and under-vehicle hydrogen tanks, Int. J. Hydrogen Energy 40 (2015) 12581–12603.

[26] Y.A. Çengel, Heat and Mass Transfer: A Practical Approach, McGraw-Hill, 2007.

[27] NIST, Isothermal properties for hydrogen, 2017, http://webbook.nist.gov/cgi/inchi?ID=C1333740&Mask=1#Thermo-Gas.

[28] F.P. Ricou, D.B. Spalding, Measurements of entrainment by axisymmetrical turbulent jets, J. Fluid Mech. 11 (1961) 21–32.

[29] J. Zheng, J. Guo, J. Yang, Y. Zhao, L. Zhao, X. Pan, J. Ma, L. Zhang, Experimental and numerical study on temperature rise within a 70 MPa type III cylinder during fast refueling, Int. J. Hydrogen Energy 38 (2013) 10956–10962.

[30] S.V. Patankar, Numerical heat transfer and fluid flow (Series in computational methods in mechanics and thermal sciences), McGraw-Hill, New York, 1980.